creative commons
COMMONS DEED

저작자표시-비영리-변경금지 2.0 대한민국

이용자는 아래의 조건을 따르는 경우에 한하여 자유롭게

- 이 저작물을 복제, 배포, 전송, 전시, 공연 및 방송할 수 있습니다.

다음과 같은 조건을 따라야 합니다:

저작자표시. 귀하는 원저작자를 표시하여야 합니다.

비영리. 귀하는 이 저작물을 영리 목적으로 이용할 수 없습니다.

변경금지. 귀하는 이 저작물을 개작, 변형 또는 가공할 수 없습니다.

- 귀하는, 이 저작물의 재이용이나 배포의 경우, 이 저작물에 적용된 이용허락조건을 명확하게 나타내어야 합니다.
- 저작권자로부터 별도의 허가를 받으면 이러한 조건들은 적용되지 않습니다.

저작권법에 따른 이용자의 권리는 위의 내용에 의하여 영향을 받지 않습니다.

이것은 이용허락규약(Legal Code)을 이해하기 쉽게 요약한 것입니다.

Disclaimer

dCollection

치의학박사학위논문

Osteogenic responses and bond strength of zirconia with hydroxyapatite coating by aerosol deposition

에어로졸 분사방식을 이용한 수산화인회석 코팅 지르코니아의 골형성 반응 및 결합강도에 관한 연구

2016년 2월

서울대학교 대학원
치의과학과 치과보철학 전공

홍 진 선

-ABSTRACT-

Osteogenic responses and bond strength of zirconia with hydroxyapatite coating by aerosol deposition

Jin-Son Hong, D.D.S., M.S.D.

Department of Prosthodontics, Graduate School, Seoul National University

(Directed by Professor **Jung-Suk Han**, D.D.S., M.S., Ph.D.)

Objectives: The purposes of this study were to evaluate the *in vitro* osteogenic potential and bonding strength of hydroxyapatite (HA)-coated zirconia by aerosol deposition method for the improved osseointegration.

Materials and Methods: Pure titanium discs (25 mm diameter, 1 mm thickness) were prepared by machining (Ti-machined; Ti-m) or treated by anodizing (Ti-anodizing; Ti-a). Green zirconia discs (15 mm diameter, 1 mm thickness) were prepared by cold isostatic pressing of the powder mixtures at 200 MPa followed by sintering for 5 h at 1650°C in air. After polishing, the (Y, Nb)-TZP and (Y, Ta)-TZP surfaces were roughened by sandblasting with 50 μm Al_2O_3 at 2 bar and 1 bar pressure, respectively. The HA by aerosol deposition to a thickness of approximately 10 μm was annealed at 700°C for 2 h under an air atmosphere. Specimens were evaluated to measure the average surface roughness (R_a) and topography by confocal laser scanning microscopy,

contact angles by automated contact-angle-measuring device, and the crystal structure by X-ray diffraction. Cell attachment was evaluated by confocal laser scanning microscope 24 h after seeding MC3T3-E1 pre-osteoblast cells on the discs. Cellular proliferation on the zirconia and titanium discs was analyzed by Picogreen assay. MC3T3-E1 pre-osteoblast cells were harvested after 2, 6, 10 and 15 days of differentiation and real-time PCR was performed to measure the expression of the bone marker genes such as type I collagen, alkaline phosphatase, and osteocalcin. Bonding strength of HA layer was evaluated by a universal testing machine and microstructure of HA coating layer was examined by scanning electron microscopy. Student t-test was used for the contact angle and R_a value. Statistical analyses for cell proliferation assay, cytotoxicity test and quantitative real time PCR were performed using one-way analysis of variance (ANOVA) with Tukey's post hoc test. Post hoc analysis was used to detect pairs of groups with statistically significance differences. Significance was considered at $p < 0.05$ (SPSS software, Chicago, IL, USA).

Results: Surface analysis by scanning electron microscopy and X-ray diffraction proved as-deposited thin HA film on the zirconia showing a shallow regular crater like surface. Deposition of dense and uniform HA-films was measured by SEM and contact angle test proved improved wettability of HA-coated surface. Confocal laser scanning microscopy indicated that MC3T3-E1 pre-osteoblasts attachment did not differ notably between the titanium and zirconia surfaces; however, cells on the HA-coated zirconia exhibited a lower proliferation than the uncoated zirconia late in the culture. Nevertheless, ALP, alizarin red S staining and bone marker gene expression analysis

indicated good osteogenic responses on HA-coated zirconia. Mean bonding strength of HA coating layer to zirconia was 26.02 MPa ± 3.92.

Conclusions: HA-coating on zirconia by aerosol-deposition improves the quality of surface modification and is favorable to the osteogenesis. Surface configuration, chemical composition of coated surface and bond strength between zirconia substrate and hydroxyapatite demonstrated that aerosol deposition method can be used as a viable option for the HA coating. However, further *in vivo* study is needed to confirm more about the efficacy of HA-coated zirconia implants with respect to osseointegration.

Key Words: Implant Dentistry, Hydroxyapatite coated zirconia, Osteogenesis, Surface chemistry, Osseointegration

Student number: 2010-31211

Osteogenic responses and bond strength of zirconia with hydroxyapatite coating by aerosol deposition

Jin-Son Hong, D.D.S., M.S.D.

Department of Prosthodontics, Graduate School, Seoul National University

(Directed by Professor **Jung-Suk Han**, D.D.S., M.S., Ph.D.)

CONTENTS

I. INTRODUCTION

Titanium (Ti) is a well-established dental implant material with many documented clinical successes [1]. Main advantageous properties of titanium are its biocompatibility and strength under bite force loading conditions; however, it produces a visible gray color in the soft tissues, making it esthetically unpleasant [2]. Consequently, tooth-colored biocompatible ceramics and bioactive glass substrates have been developed as novel candidate implant materials [3]. Zirconia (Zr) is one of the most widely used ceramic implants, because its material properties are biocompatible *in vitro* and *in vivo*, osteoconductive and chemically inert. Moreover, the color of zirconia matches natural teeth tint [4]. Pure zirconia is monoclinic at room temperature, but as the temperature increases, zirconia transforms to a tetragonal structure by approximately 1,170℃ and then to a cubic structure about 2,370℃. As the temperature decreases 4.5% volume changes occurs from tetragonal to monoclinic phase transformation. There have been many trials to achieve the stability at the room temperature using phase stabilizers such as CaO, MgO, and Y_2O_3. Y_2O_3-stabilized tetragonal zirconia polycrystals (Y-TZP) have several advantages over other ceramics, including high fracture toughness and flexural strength [5], and were widely used for hip replacements. However, reports of clinical failures caused by low-temperature degradation (LTD) indicated a need to improve the structural stability of this material [6, 7]. Modifications of zirconia with tantalum oxide (Ta_2O_5) or niobium oxide (Nb_2O_5) have been developed to prevent LTD [8, 9]. Tetragonal zirconia polycrystal (TZP) containing Y_2O_3/Ta_2O_5 or Y_2O_3/Nb_2O_5 [(Y, Ta)-TZP and (Y, Nb)-TZP, respectively] had a similar osteogenic potential to those grown

on anodized titanium, which is widely used as a dental implant material [10]. Material composition and surface topography are critical modulators of osseointegration. Accordingly, various surface modifications have been developed to enhance bone healing, including mechanical modifications such as grooves or textured rough patterns [11, 12, 13] and coating with biomaterials or biomolecules to induce osteogenesis [14, 15, 16, 17].

HA is the natural mineral form of calcium apatite, the main component of bones and teeth. Therefore, it is widely accepted as a graft material for the treatment of bone defects and as a coating material to promote osteogenesis. The advantages of hydroxyapatite coated dental implant include rapid fixation and stronger bonding between bone and implant and increased uniform bone ingrowth at the bone-implant interface. Thus, HA was the first material used for osseointegration in dental implants [17, 18, 19, 20], although its use is controversial because HA-coated implants have been poorly characterized. There are some concerns about the use of HA coating in dental implant. One of important concerns is the resorption a degradability of HA coating in a biological environment, which could lead to disintegration of the coating, resulting in the loss of both the coating-substrate bond strength and the implant fixation [20, 21]. Furthermore, poor-quality coatings limit the utility of HA, causing failures in bone healing and implantation. HA surface-coating methods include electrophoretic deposition, dip coating and spin coating, immersion coating, hot isostatic pressing, solution deposition, sputter coating and thermal spraying such as plasma spraying, flame spraying and high-velocity oxy-fuel combustion spraying [22, 23, 24, 25]. However, the only used coating method for titanium dental implants in clinical practice

is the plasma spraying technique. Advantages of plasma spraying method include a rapid deposition rate and sufficiently low cost. Unfortunately there are disadvantages in the plasma-spraying method such as the porosity of the coating, residual stress at the interface between the substrate and coating materials and drastic changes in the composition and crystallinity of the initial HA powder. These causes variation in bond strength between the coating and substrate, alterations in HA structure due to coating process, and poor adhesion at the interface between the coating and substrate [21]. Moreover, the plasma-spraying method is not effective for coating small dental implants with a complex shape [26].

It is difficult to produce a crystalline HA-coated surface with controlled pore size and porosity. In this study, an aerosol deposition technique was introduced to produce a high-quality HA-coating on zirconia surfaces and supplemented the drawbacks of HA-coating. The aerosol deposition technique is a form of gas deposition method with no need of vaporization of the raw material [27, 28]. The aerosol deposition method is a spray coating process to produce high quality dense ceramic films from an initial raw powder at room temperature on the substrate material without sintering [29].

The objective of this study is to evaluate surface characteristics of HA-coated zirconia surface using a novel aerosol deposition technique and osteogenic responses to the HA-coated zirconia.

II. MATERIALS AND METHODS

2. 1 Specimen preparation

Pure titanium discs (25 mm diameter, 1 mm thickness) were prepared by machining (Ti-machined; Ti-m) or treated by anodizing (Ti-anodizing; Ti-a) (OnePlant System, Warrantec, Seoul, Korea). Zirconia was prepared by mixing 90.6 mol% ZrO_2, 5.3 mol% Y_2O_3, and 4.1 mol% Nb_2O_5 powders for (Y, Nb)-TZP, and 86.2 mol% ZrO_2, 7.2 mol% Y_2O_3, and 6.6 mol% Ta_2O_5 for (Y, Ta)-YZP. The compositions were selected on the basis of absence of the low temperature degradation and reasonably high fracture toughness. Green zirconia discs (15 mm diameter, 1 mm thickness) were prepared by cold isostatic pressing of the powder mixtures at 200 MPa followed by sintering for 5 h at 1650°C in air. The zirconia discs were polished and finished with diamond pastes to generate a mirror-like surface. After polishing, the (Y, Nb)-TZP and (Y, Ta)-TZP surfaces were roughened by sandblasting with 50 μm Al_2O_3 at 2 bar and 1 bar pressure, respectively.

2.2 Fabrication of HA film using aerosol deposition

Commercially available HA powder (CodeBio, Cheonan, Korea) was used as the starting raw material for aerosol deposition (AD). The HA was annealed at 700°C for 2 h under an air atmosphere. Sandblasted (Y, Nb)-TZP and (Y, Ta)-TZP were ultrasonically cleaned with distilled water and acetone. The equipment used for AD of HA was primarily composed of an aerosol chamber and a processing chamber, connected by a tube (Fig. 1). Preheated HA powders were mixed with carrier gas and

aerosolized using a vibration system. The aerosol was added to the coating chamber through the tube and accelerated through a slit nozzle by pressure differences between the two chambers. The accelerated HA powder was ejected from the slit nozzle and deposited onto the discs at room temperature, to a thickness of approximately 10 μm.

2.3 Surface roughness and interface

The average surface roughness (R_a) and topography were measured by confocal laser scanning microscopy (CLSM; LSM700, Carl Zeiss, Oberkochen, Germany). The microstructure of the zirconia discs with and without HA-coating was observed by scanning electron microscopy (SEM; SNE-4500M, SEC CO., LTD, Suwon, Korea). In addition to this, interface between HA-films and zirconia discs were observed by SEM to confirm deposition of dense HA-films. R_a values represent the mean ± SD of three independent experiments.

2.4 Contact angle

Four uncoated zirconia discs and HA-coated zirconia discs were prepared. Distilled water at 36.5ºC was dropped onto each of the discs, and 5 seconds later contact angles were measured using an automated contact-angle-measuring device (Pheonix300, S.E.O. Co., Ltd. Ansung, Korea). Values represent the mean ± SD of three independent experiments.

2.5 Crystallinity

X-ray diffraction (XRD; MiniFlex 600; Rigaku CO., LTD, Tokyo, Japan) was used to

examine the crystal structure of the deposited HA-layer. XRD data was matched with Joint Committee on Powder Diffraction Standards (JCPDS) card # 9-432.

2.6 Cell culture

Mouse pre-osteoblast MC3T3-E1 cells were purchased from ATCC (Manassas, VA, USA), seeded on the discs, and cultured in α-minimal essential medium (α-MEM, Logan, UT, USA) with 10% fetal bovine serum (FBS) and 1% penicillin/streptomycin. Trypsinized and resuspended cells seeded on the discs at a density $1x10^4$ cells/cm^2 and incubated in air at 37°C and 5% CO_2. Three specimens were statically cultured per time interval and 3 sets of cultures were examined for all *in vitro* experiments. The osteogenic medium contained 10 mM β-glycerophosphate and 50 μg/mL ascorbic acid in the α-MEM.

2.7 Cell attachment

Twenty-four hours after seeding, disc-adherent cells were fixed in 4% formaldehyde. 4′, 6-Diamidino-2-phenylindole (DAPI; Invitrogen, Carlsbad, CA, USA), and Alexa Fluor 568 phalloidin (Invitrogen, Carlsbad, CA, USA) were used for detection of the nucleus and cytoskeleton, respectively. Fluorescence was visualized by CLSM and analyzed with ZEN2011 software (Carl Zeiss, Oberkochen, Germany).

2.8 Cell proliferation assay

Picogreen assays were performed with a Quant-iT Picogreen assay kit (Invitrogen Ltd.,

Paisley, UK) at 1, 4 and 7 days after seeding following attachment to assess cellular proliferation. MC3T3-E1 cells ($1x10^4$ cells/cm^2) were seeded on the discs. Disc-adhered cells were washed with phosphate-buffered saline (PBS) and lysed with TE buffer (10 mM Tris-HCl, 1 mM EDTA, pH 7.5). DNA contents were determined by mixing 100 μL of Picogreen reagent with 100 μL of DNA sample. The samples were loaded in triplicate and fluorescence intensity was measured with a GloMax Multi-Detection System (Promega, Madison, WI, USA). Fluorescence intensity was converted to DNA concentration using a DNA standard curve according to the manufacturer's protocol. Values represent the mean ± SD of three independent experiments.

2.9 Cytotoxicity test

Cytotoxicity was measured using Cell Counting Kit-8 (CCK-8; Dojindo, Tokyo, Japan). MC3T3-E1 cells ($1x10^4$ cells/cm^2) were plated on the discs and tests were performed at 1, 4 and 7 days after seeding. CCK-8 solution was added to each well and followed by incubation for 2 h at 37°C. The absorbance at 450 nm was determined by a GloMax Multi-Detection System (Promega, Madison, WI, USA). Values represent the mean ± SD of three independent experiments.

2.10 Reverse-transcription PCR and quantitative real-time PCR

Cells were harvested at 2, 6, 10 and 15 days after osteoblast differentiation. RNA was isolated with QIAzol lysis reagent (QIAGEN, Valencia, CA, USA). The Primescript™ RT reagent kit for reverse transcription was purchased from Takara (Shiga, Japan). Quantitative real-time PCR was performed with primer sets for type I collagen

(*Col1A1*), alkaline phosphatase (*Alp*) and osteocalcin (*Oc*) and with Takara SYBR premix Ex Taq (Takara) on an 7500 Real-Time PCR system (Applied Biosystems, Foster City, CA, USA). The PCR primers were synthesized by Integrated DNA Technology (Coralville, IA, USA). All samples were run in duplicate and the relative expression levels were normalized to glyceraldehyde-3-phosphate dehydrogenase (*Gapdh*). *Gapdh* mRNA expression levels remained steady during osteoblasts differentiation showing similar Ct value. Values represent the mean ± SD of three independent experiments.

2.11 Alkaline phosphatase (ALP) staining

An ALP staining kit was purchased from Sigma-Aldrich (St. Louis, MO, USA). Cells were cultured in osteogenic medium for 7 days, washed twice with PBS, and stained as described by the manufacturer.

2.12 Alizarin red S staining

Cells were cultured in osteogenic medium for 21 days and washed twice with PBS, fixed with 70% ethanol for 1 h, washed twice with distilled water, and stained with 40 mM alizarin red S (Sigma-Aldrich, St. Louis, MO, USA) for 10 min, then washed three times with distilled water.

2.13 Bonding strength

Cylindrical shape zirconia specimens (8mm in diameter x 25mm in length) were

fabricated. Cone shape top (4mm in diameter) in the specimen for bonding strength test was milled. HA layer on the top was coated by the aerosol deposition technique as previously mentioned. Thickness of the HA layer was approximately 5㎛. Specimens with HA coating layer were glued to the zirconia substrate using FM 1000 Adhesive Film (Cytec 751, Cytec Engineered Materials Inc., USA) (Fig. 2). The couples were put into an preheated oven at 176℃ for 3 hours, and then cooled down to the room temperature. The specimens were loaded into the universal testing machine (Instron 3365, Instron Co., USA) with jig. Tensile load was applied to the specimens at a constant cross-head speed of 2.5mm/min until fracture occurred. The data for bonding strength was reported as the average of values. The fractured surfaces of the substrates and HA layer were observed by scanning electron microscopy (SEM; JEOL JSM-6390, JEOL CO., USA).

2.14 Statistical analysis

All quantitative data are presented as the mean ± SD. Each experiment was performed at least three times, and the results from one representative experiment are shown. Student t-test was used for the contact angle and R_a value. Statistical analyses for cell proliferation assay, cytotoxicity test and quantitative real time PCR were performed using one-way analysis of variance (ANOVA) with Tukey's post hoc test. Post hoc analysis was used to detect pairs of groups with statistically significance differences. Significance was considered at $p < 0.05$ (SPSS software, Chicago, IL, USA).

III. RESULTS

3.1 Characterization of the HA film

HA film was produced and optimized using HA powder with a particle size of approximately 0.8–1.1 μm. The XRD patterns of the raw HA powder before deposition (raw), the heat-treated HA powder (700^{o}C), and the as-deposited HA film (as-deposited) are shown in Fig. 3A (labeled a, b, and c, respectively). The peaks of the HA powder were consistent with the dominant peaks of pure HA with high crystallinity (asterisk, Fig. 3A). XRD analysis revealed only HA peaks (JCPDS cards # 9-432). Collectively, the HA film exhibited only pure HA peaks without secondary crystalline phases. Thus, the composition of the powder and film indicated that no chemical changes had occurred during deposition. The cross-section of HA films on the (Y, Nb)-TZP (a) and (Y, Ta)-TZP (b) was observed by SEM (Fig. 3B). There were no pore and crack in the film layers, indicating the deposition of the fully dense HA films. The deposited HA films had no orientation and showed the round shaped particles because the raw HA particles for an aerosol deposition were round. The thickness of HA films was averagely 8.05 and 8.70 μm on (Y, Nb)-TZP and (Y, Ta)-TZP discs and the thickness of all experiment specimens was well maintained in this study. The contact angle was significantly lower for HA-coated surface (a, 63.72 ± 2.55˚, $P<0.001$; Fig. 3C) than for non-coated zirconia surface (b, 95.0 ± 3.21º, $P<0.001$; Fig. 3C).

3.2 Surface analysis of HA film on zirconia by AD

For each specimen, the average roughness (R_a) and surface topography were analyzed

by CLSM. The R_a values of the (Y, Nb)-TZP and HA-coated (Y, Nb)-TZP were 0.819 ± 0.05 μm and 1.131 ± 0.12 μm, respectively (Fig. 4A and B, upper panel). The R_a values of the (Y, Ta)-TZP and HA-coated (Y, Ta)-TZP surfaces were 0.880 ± 0.06 μm and 1.004 ± 0.12 μm, respectively (Fig. 4C and D, upper panel). Significant increase was observed in surface roughness with HA coating ($p<0.05$). The surface morphology was observed by SEM (Fig. 4A-D, bottom panel). As-deposited HA film on the discs produced a shallow crater like surface with a network-type microstructure (Figs. 4B and 4D, bottom panel) and increased surface roughness.

3.3 Cell attachment and morphology

Cell attachment and morphology were examined by CLSM 24 h after seeding MC3T3-E1 pre-osteoblast cells on the discs (Fig. 5). Cell adhesion to the (Y, Nb)-TZP (Fig. 5C) and (Y, Ta)-TZP (Fig. 5E) discs was similar to adhesion to the Ti-m (Fig. 5A) and Ti-a (Fig. 5B) discs. However, cells on the HA-coated (Y, Nb)-TZP (Fig. 5D) and HA-coated (Y, Ta)-TZP (Fig. 5F) discs exhibited unusual morphology with an elongated and thin cytoskeletal appearance.

3.4 Cellular proliferation and viability

Cellular proliferation on the zirconia and titanium discs was analyzed by Picogreen assay (Fig. 6A). Cells were seeded and cultured on the discs and harvested at 1, 4 and 7 days. The proliferation was increased throughout the experiment; cells proliferated more efficiently on the polished surfaces (Ti-m) than on the rough surfaces [Ti-a, (Y, Nb)-TZP

± HA, and (Y, Ta)-TZP ± HA]. Although the cell morphology suggested otherwise, cells on the HA-coated zirconia discs proliferated well, although more slowly than those on the uncoated discs. CCK-8 assay was also tried for the cell viability, and it was agreed with the results of Picogreen assay (Fig. 6B). These results suggest the HA coating is not cytotoxic; thus, it is biocompatible.

3.5 Osteoblast differentiation

MC3T3-E1 pre-osteoblast cells were harvested after 2, 6, 10 and 15 days of differentiation and real-time PCR was performed to measure the expression of the bone marker genes *Col1A1* (Fig. 7A), *Alp* (Fig. 7B), and *Oc* (Fig. 7C). Although the osteoblast differentiation patterns were similar, the degree of differentiation varied slightly among the surfaces. The polished Ti-m surface had a lower differentiation capacity than the rough surfaces (Ti-a). Notably, HA-coated (Y, Nb)-TZP and HA-coated (Y, Ta)-TZP exhibited osteogenic responses that were equivalent or slightly high to that of Ti-a, which is well known for its efficacy in dental osseointegration. To verify the osteogenic effects of HA-coated zirconia, we performed ALP staining (Fig. 7D) and alizarin red S staining (Fig. 7E), which showed that the HA-coated (Y, Nb)-TZP and HA-coated (Y, Ta)-TZP discs have some better osteogenic potentials than the uncoated zirconia discs.

3.6 Bonding strength

Tensile bonding strengths of the HA coating layer to zirconia were measured by ASTM

F1147-05 method. The mean bonding strength of each specimen was 26.02 MPa ± 3.92 (Fig. 8A). From the SEM photographs of the fractured surfaces, HA residues were observed on the zirconia surface coatings (Fig. 8B). This indicates that the fracture occurred mainly at the HA-film interface, leaving the HA remaining on the zirconia surface. The failure modes were a combination of adhesive between HA coating and zirconia and cohesive failure within the HA coating layer.

IV. DISCUSSION

In this study, novel method for depositing HA film by aerosol deposition (AD) was presented. HA-coating was first introduced in the 1980s for the improved osseointegration between bone and implant [30]. Many studies have been focused on the osteogenic response to HA-coating interface, furthermore, on the problems associated with the coating method and optimization of coating properties for the best biocompatibility and osseointegration [20, 22, 31]. Several HA-coating methods were introduced. Among them, plasma spraying is commercially the most frequently used method and showed many advantages about the bone tissue response. However, despite the successful results, it showed also disadvantages such as irregularity in thickness, variations in crystallinity and composition of the coating, and exfoliation of coating layer. Therefore, it is important to ensure whether the coating layer is uniform, and crystallinity or composition is not changed.

Surface analysis in the present study confirmed that the specimens had uniform and dense HA-coating thickness, improved wettability and improved surface roughness. XRD data showed slightly weaker and broadened HA peaks of the films in comparison to the original HA powder (Fig. 3A). The presence of weak, broadened XRD peaks might suggest a small crystallite size of the coating; however, it is well known that these phenomena can be induced by the high-energy impact of the powder particles on the substrate during the AD process [28]. In the present study, HA-coating layer is composed of dense and uniform crystalline without a creation of amorphous HA, and hence it can be suggested that aerosol deposition will be highly resistant to dissolution what is drawback of HA-coating. Surface energy can be evaluated by measuring contact

angles as a primary indicator of potential cellular adhesion and implant surface biocompatibility [21]. Moreover, the surface hydrophilicity has been known to influence osseointegration. HA-coating in this study reduced the contact angle significantly and induced hydrophilicity (Fig. 3C). As is well known, rapid hydration of the surface could enhance the cell adhesion and bone apposition [32]. Therefore, it could be suggested that the data from this study with enhanced wettability in the HA-coated surface would have a good influence on the osseointegration. Many review articles reported about the positive relationship between surface roughness and osseointegration [26, 33, 34]. Based on these, many trials for making suitable surface roughness were introduced including HA-coating. SEM data showed that the HA-coating formed a rough surface with a porous network-type microstructure and improved the R_a value of the zirconia discs (Fig. 4).

Excellent osseointegration is the final goal of bone tissue healing around implant materials. HA must induce an appropriate cellular response to ensure biocompatibility and bioactivity and to promote osseointegration between bone and implant with good quality coating. In this study, HA-deposition induced a slight stress response in adhered cells, observed as a debulked and elongated cytoskeleton (Figs. 5D and F). Moreover, while HA did not affect proliferation at 4 day of cell culture, proliferation was slightly lower than on the uncoated surfaces by day 7 (Fig. 6). This apparent phenomenon has been demonstrated elsewhere *in vitro*, whereas an *in vivo* study showed early tissue integration [35]. Despite the slight stressful state was observed on the HA-coated zirconia in the present study (Fig. 5 and 6), real-time PCR and staining showed that the cells well differentiated on HA-coated zirconia surface (Fig. 7). Many other *in vitro* and

in vivo studies have reported the benefits of HA deposition on implants [36, 37, 38]; however, HA coatings also present problems such as dissolution of the HA and bacterial susceptibility [20].

Many studies reported that HA coating to titanium implant by plasma-spraying method showed low adhesion between HA coating and substrate, which caused failures in bone healing and implantation. There were many effort to improve the bonding strength of HA coating by forming a various composite coating with titanium and heat treatment [39, 40, 41]. But the bonding strengths of HA coating to titanium reported in the previous studies were less than 20 MPa [39, 41]. In this study, the bonding strength of HA coating to zirconia was higher than that of HA coating to titanium.

Thus, improving the clinical usefulness of HA in dental implant materials remains a priority for the future studies. Taken together, a novel HA-coating method by aerosol deposition in this study can be used to apply a thin and uniform coating of highly crystalline HA over zirconia implants with good wettability. Furthermore, this *in vitro* study demonstrated that HA-coating could be used for the method of implant surface modification showing favorable osteogenic response.

V. CONCLUSIONS

Within the limits of this experimental study, the following conclusions can be drawn:

1. No chemical changes in the HA coating occurred by aerosol deposition method.
2. The contact angle was significantly lower for HA-coated zirconia surface than for non-coated zirconia surface.
3. Significant increase was observed in surface roughness with HA coating zirconia surface.
4. Cell attachment to the zirconia surface was similar to adhesion to that of titanium discs.
5. HA-coated zirconia showed osteogenic responses that were equivalent or slightly high to that of titanium.
6. Mean bonding strength of HA coating layer to zirconia was 26.02 MPa ± 3.92.

Zirconia with HA-coating by aerosol-deposition improves the quality of surface modification and is favorable to the osteogenesis. However, further *in vivo* study is needed to confirm more about the efficacy of HA-coated zirconia implants with respect to osseointegration.

REFERENCES

[1] Buser D, Janner SF, Wittneben JG, Bragger U, Ramseier CA, Salvi GE. 10-year survival and success rates of 511 titanium implants with a sandblasted and acid-etched surface: a retrospective study in 303 partially edentulous patients. *Clin Implant Dent Relat Res* 2012;14:839-851.

[2] Sailer I, Zembic A, Jung RE, Hammerle CH, Mattiola A. Single-tooth implant reconstructions: esthetic factors influencing the decision between titanium and zirconia abutments in anterior regions. *Eur J Esthet Dent* 2007;2:296-310.

[3] Kaur G, Pandey OP, Singh K, Homa D, Scott B, Pickrell G. A review of bioactive glasses: Their structure, properties, fabrication, and apatite formation. *J Biomed Mater Res A* 2014;102:254-274.

[4] Hisbergues M, Vendeville S, Vendeville P. Zirconia: Established facts and perspectives for a biomaterial in dental implantology. *J Biomed Mater Res B Appl Biomater* 2009;88:519-529.

[5] Pittayachawan P, McDonald A, Young A, Knowles JC. Flexural strength, fatigue life, and stress-induced phase transformation study of Y-TZP dental ceramic. *J Biomed Mater Res B Appl Biomater* 2009;88:366-377.

[6] L Gremillard JC. Durability of zirconia-based ceramics and composites for total hip replacement. *Key Engineering Materials* 2008;361:791~794.

[7] Lughi V, Sergo V. Low temperature degradation -aging- of zirconia: A critical review of the relevant aspects in dentistry. *Dent Mater* 2010;26:807-820.

[8] Kim DJ, Lee MH, Lee DY, Han JS. Mechanical properties, phase stability, and biocompatibility of (Y,Nb)-TZP/Al2O3 composite abutments for dental implant. *J Biomed Mater Res* 2000;53:438-443.

[9] Piconi C, Maccauro G. Zirconia as a ceramic biomaterial. *Biomaterials* 1999;20:1-25.

[10] Cho YD, Shin JC, Kim HL, Gerelmaa M, Yoon HI, Ryoo HM. Comparison of the osteogenic potential of titanium- and modified zirconia-based bioceramics. *Int J Mol Sci* 2014;15:4442-4452.

[11] Gahlert M, Gudehus T, Eichhorn S, Steinhauser E, Kniha H, Erhardt W. Biomechanical and histomorphometric comparison between zirconia implants with varying surface textures and a titanium implant in the maxilla of miniature pigs. *Clin Oral Implants Res* 2007;18:662-668.

[12] Hsu SH, Liu BS, Lin WH, Chiang HC, Huang SC, Cheng SS. Characterization and biocompatibility of a titanium dental implant with a laser irradiated and dual-acid etched surface. *Biomed Mater Eng* 2007;17:53-68.

[13] Orsini G, Assenza B, Scarano A, Piattelli M, Piattelli A. Surface analysis of machined versus sandblasted and acid-etched titanium implants. *Int J Oral Maxillofac Implants* 2000;15:779-784.

[14] Aldini NN, Fini M, Giavaresi G, Torricelli P, Martini L, Giardino R. Improvement in zirconia osseointegration by means of a biological glass coating: An in vitro and in vivo investigation. *J Biomed Mater Res* 2002;61:282-289.

[15] Burr DB, Mori S, Boyd RD, Sun TC, Blaha JD, Lane L. Histomorphometric

assessment of the mechanisms for rapid ingrowth of bone to HA/TCP coated implants. *J Biomed Mater Res* 1993;27:645-653.

[16] De Maeztu MA, Braceras I, Alava JI, Gay-Escoda C. Improvement of osseointegration of titanium dental implant surfaces modified with CO ions: a comparative histomorphometric study in beagle dogs. *Int J Oral Maxillofac Surg* 2008;37:441-447.

[17] Knabe C, Howlett CR, Klar F, Zreiqat H. The effect of different titanium and hydroxyapatite-coated dental implant surfaces on phenotypic expression of human bone-derived cells. *J Biomed Mater Res A* 2004;71:98-107.

[18] Mistry S, Kundu D, Datta S, Basu D, Soundrapandian C. Indigenous hydroxyapatite coated and bioactive glass coated titanium dental implant system - Fabrication and application in humans. *J Indian Soc Periodontol* 2011;15:215-220.

[19] Ogiso M, Tabata T, Ichijo T, Borgese D. Examination of human bone surrounded by a dense hydroxyapatite dental implant after long-term use. *J Long Term Eff Med Implants* 1992;2:235-247.

[20] Sun L, Berndt CC, Gross KA, Kucuk A. Material fundamentals and clinical performance of plasma-sprayed hydroxyapatite coatings: a review. *J Biomed Mater Res* 2001;58:570-592.

[21] Ong JL, Chan DC. Hydroxyapatite and their use as coatings in dental implants: a review. *Crit Rev Biomed Eng* 2000;28:667-707.

[22] Han JY, Yu ZT, Zhou L. Hydroxyapatite/titania composite bioactivity coating

processed by the sol-gel method. *Biomed Mater* 2008;255:455-458.

[23] Kuroda K, Ichino R, Okido M, Takai O. Hydroxyapatite coating on titanium by thermal substrate method in aqueous solution. *J Biomed Mater Res* 2002;59:390-397.

[24] Lee J, Aoki H. Hydroxyapatite coating on Ti plate by a dipping method. *Biomed Mater Eng* 1995;5:49-58.

[25] Tamura M, Endo K, Maida T, Ohno H. Hydroxyapatite film coating by thermally induced liquid-phase deposition method for titanium implants. *Dent Mater* 2006;25:32-38.

[26] Le Guehennec L, Soueidan A, Layrolle P, Amouriq Y. Surface treatments of titanium dental implants for rapid osseointegration. *Dent Mater* 2007;23:844-854.

[27] Akedo J, Lebedev M. Piezoelectric properties and poling effect of Pb(Zr, Ti)O-3 thick films prepared for microactuators by aerosol deposition. *Appl Phys Lett* 2000;77:1710-1712.

[28] Akedo J. Aerosol deposition of ceramic thick films at room temperature: Densification mechanism of ceramic layers. *J Am Ceram Soc* 2006;89:1834-1839.

[29] Hanft D, Exner J, Schubert M, Stcker T, Fruierer P, Moos R. An overview of the aerosol deposition method: process fundamentals and new trends in materials applications. *J Ceram Sci Tech* 2015;6:147-182

[30] Furlong RJ, Osborn JF. Fixation of hip prostheses by hydroxyapatite ceramic coatings. *J Bone Joint Surg Br* 1991;73:741-745.

[31] Wang H, Eliaz N, Xiang Z, Hsu HP, Spector M, Hobbs LW. Early bone apposition in vivo on plasma-sprayed and electrochemically deposited hydroxyapatite coatings on titanium alloy. *Biomaterials* 2006;27:4192-4203.

[32] Rupp F, Scheideler L, Olshanska N, de Wild M, Wieland M, Geis-Gerstorfer J. Enhancing surface free energy and hydrophilicity through chemical modification of microstructured titanium implant surfaces. *J Biomed Mater Res A* 2006;76:323-334.

[33] Shalabi MM, Gortemaker A, Van't Hof MA, Jansen JA, Creugers NH. Implant surface roughness and bone healing: a systematic review. *J Dent Res* 2006;85:496-500.

[34] Wennerberg A, Albrektsson T. On Implant Surfaces: A review of current knowledge and opinions. *Int J Oral Maxillofac Implants* 2010;25:63-74.

[35] Roy M, Bandyopadhyay A, Bose S. Induction of plasma sprayed nano hydroxyapatite coatings on titanium for orthopaedic and dental implants. *Surf Coat Technol* 2011;205:2785-2792.

[36] Chang YL, Stanford CM, Wefel JS, Keller JC. Osteoblastic cell attachment to hydroxyapatite-coated implant surfaces in vitro. *Int J Oral Maxillofac Implants* 1999;14:239-247.

[37] Rigo ECS, Boschi AO, Yoshimoto M, Allegrini S, Konig B, Carbonari MJ. Evaluation in vitro and in vivo of biomimetic hydroxyapatite coated on titanium dental implants. *Materials Science & Engineering C-Biomimetic and Supramolecular Systems* 2004;24:647-651.

[38] Yang GL, He FM, Hu JA, Wang XX, Zhao SF. Effects of biomimetically and

electrochemically deposited nano-hydroxyapatite coatings on osseointegration of porous titanium implants. *Oral Surg Oral Med Oral Pathol Oral Radiol Endod* 2009;107:782-789.

[39] Zheng X, Huang M, Ding C. Bond strength of plasma-sprayed hydroxyapatite/Ti compoiste coatings. *Biomaterials* 2000;21:841-849.

[40] Yang YC, Chou BY. Bonding strength investigation of plasma-sprayed HA coatings on alumina substrate with porcelain intermediate layer. *Mater Chem Phys* 2007;104:312-319.

[41] Yang YC, Chang E. Influence of residual stress on bonding strength and fracture of plasma-sprayed hydroxyapatite coatings on Ti-6Al-4V substrate. *Biomaterials* 2001;22:1827-1836.

FIGURES

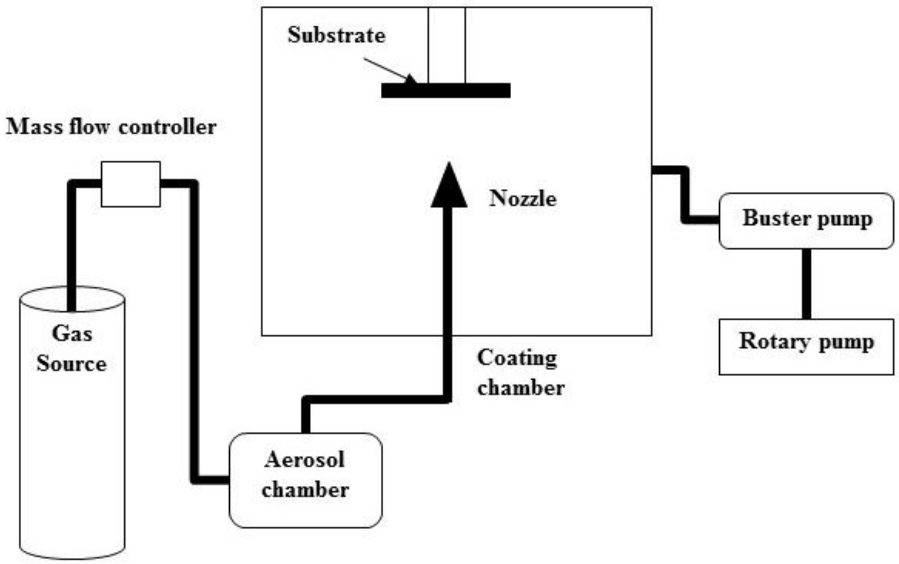

Fig. 1. Schematic diagram of the aerosol deposition process

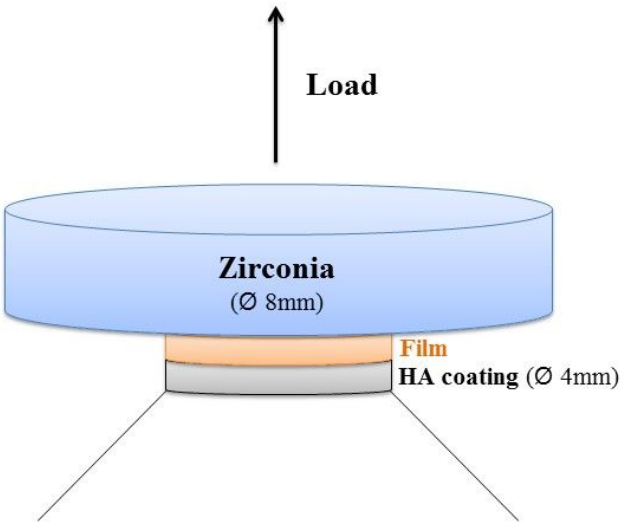

Fig. 2. Schematic diagram of the tensile bond strength test

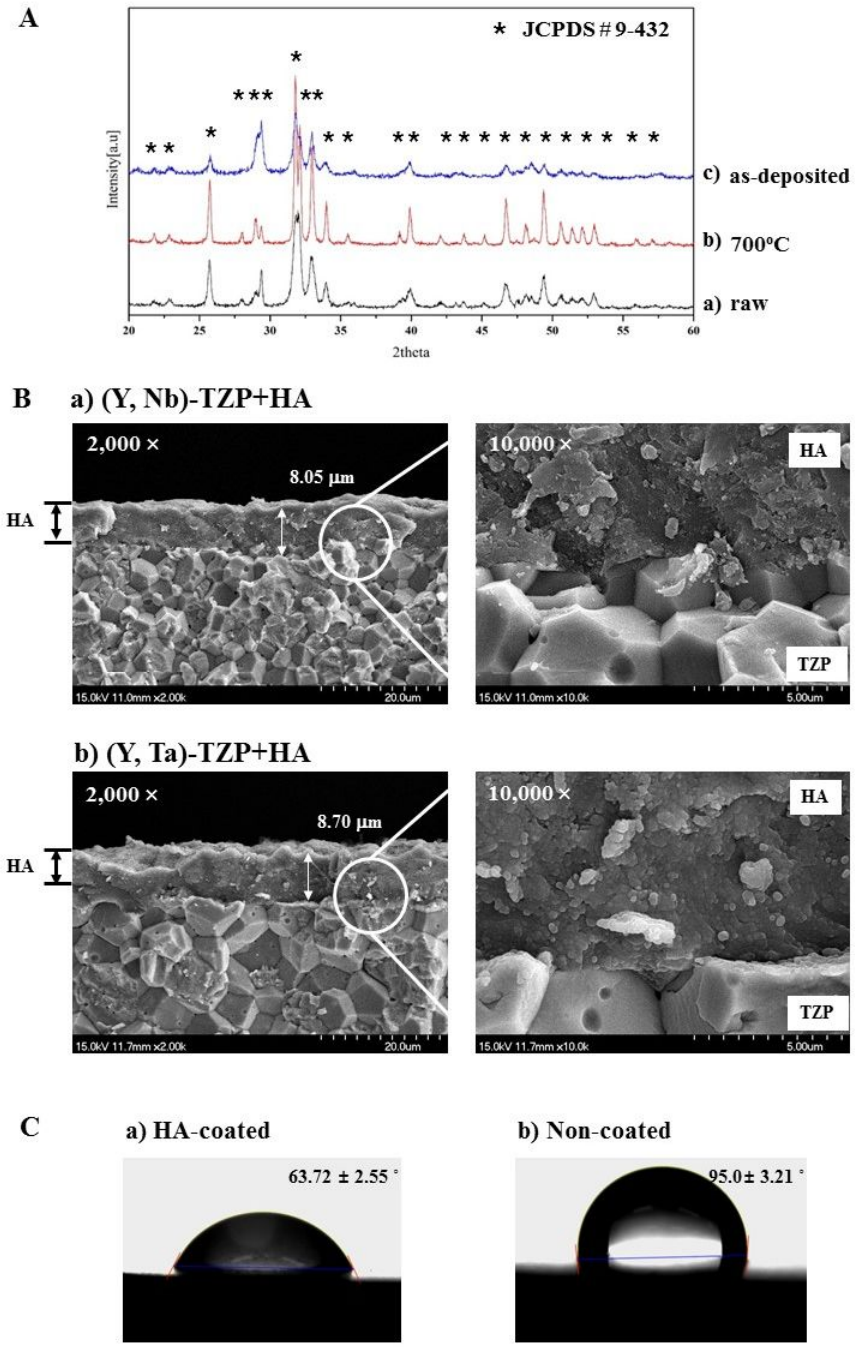

Fig. 3. A. XRD patterns of raw HA powder before deposition (a), heat-treated HA powder (b), and as-deposited HA film (c) on the zirconia discs. B. The cross-sections of the deposited HA-film (HA-coated (Y, Nb)-TZP (a) and HA-coated (Y, Ta)-TZP (b)) were observed using SEM. Images are magnified 2000× (left) and 10,000× (right). C. Contact angle between the water drop and the substratum: (a) HA-coated zirconia surface, (b) non-coated zirconia surface.

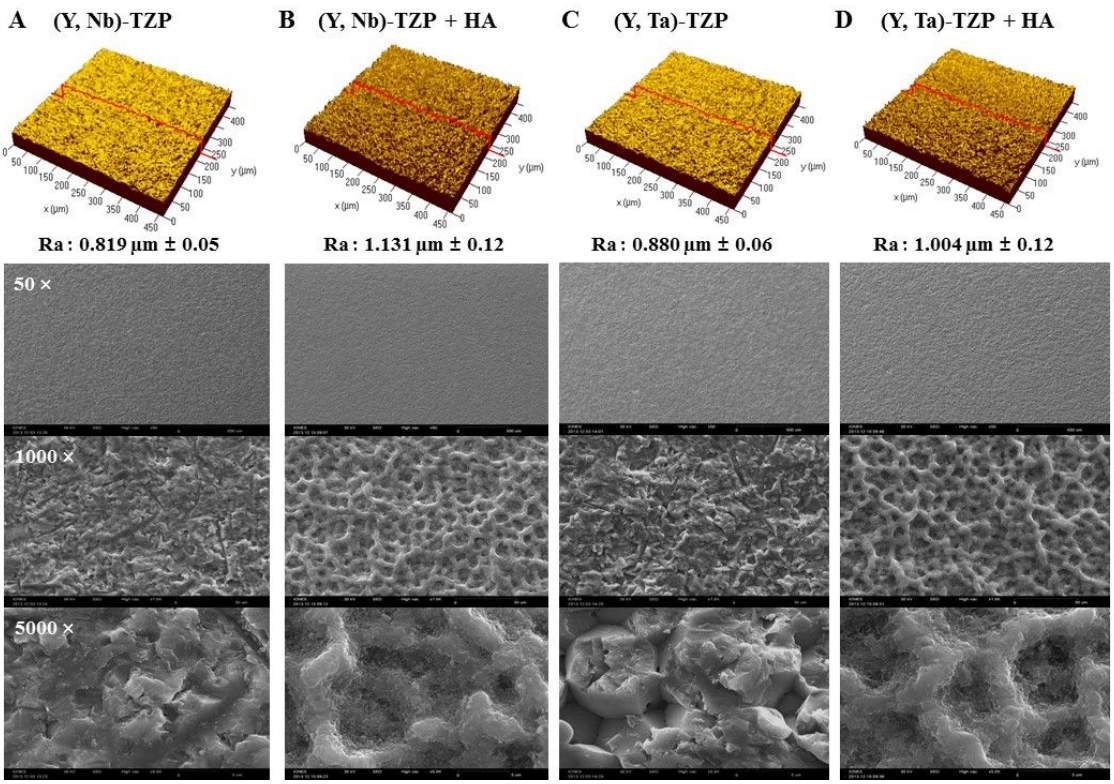

Fig. 4. CLSM images showing the roughness (R_a) of the material surfaces (upper panel) A. (Y, Nb)-TZP; B. HA-coated (Y, Nb)-TZP; C. (Y, Ta)-TZP; D. HA-coated (Y, Ta)-TZP. SEM images of material surfaces (A-D, bottom panel). Images are magnified 50×, 1000×, and 5000×.

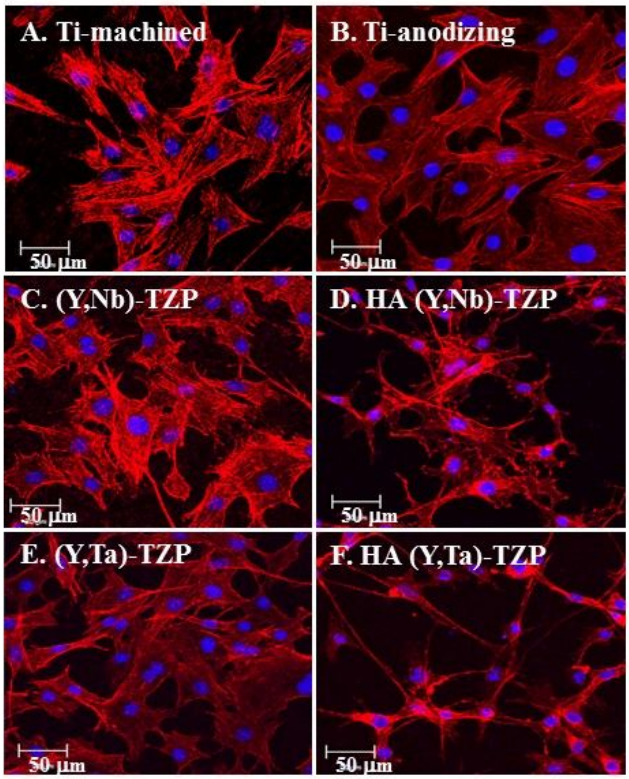

Fig. 5. Confocal images of MC3T3-E1 cells 24 h after seeding on Ti or Zr discs. A. Titanium-machined, B. Titanium-anodizing, C. Sandblasted (Y, Nb)-TZP, D. HA-coated (Y, Nb)-TZP, E. Sandblasted (Y, Ta)-TZP, F. HA-coated (Y, Ta)-TZP. Original magnification is 300×; bar = 50 μm.

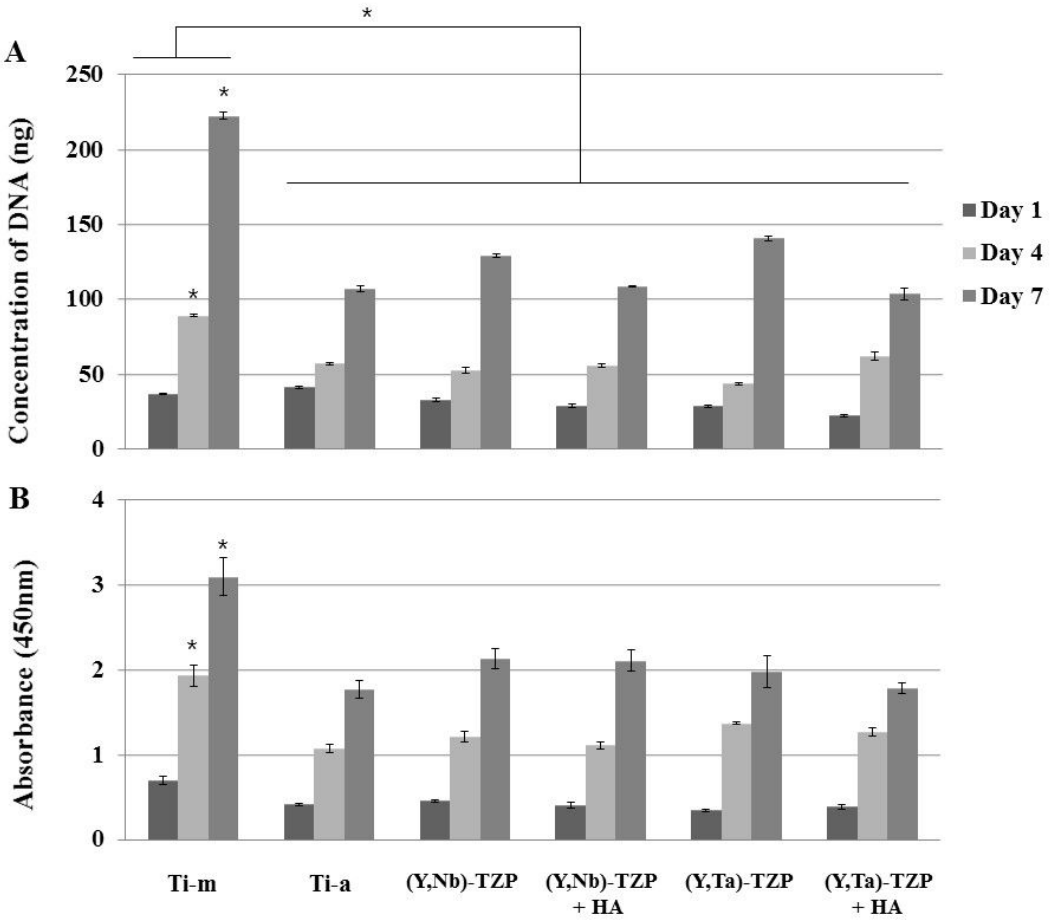

Fig. 6. A. Picogreen assay. Proliferation of MC3T3-E1 cells on Ti or Zr discs on days 1, 4 and 7. B. CCK-8 assay. Cell viability was tested on days 1, 4, and 7 with the same condition with Picogreen assay. The data are expressed as the mean ± SD of three independent experiments. * Significant differences between groups ($p < 0.05$).

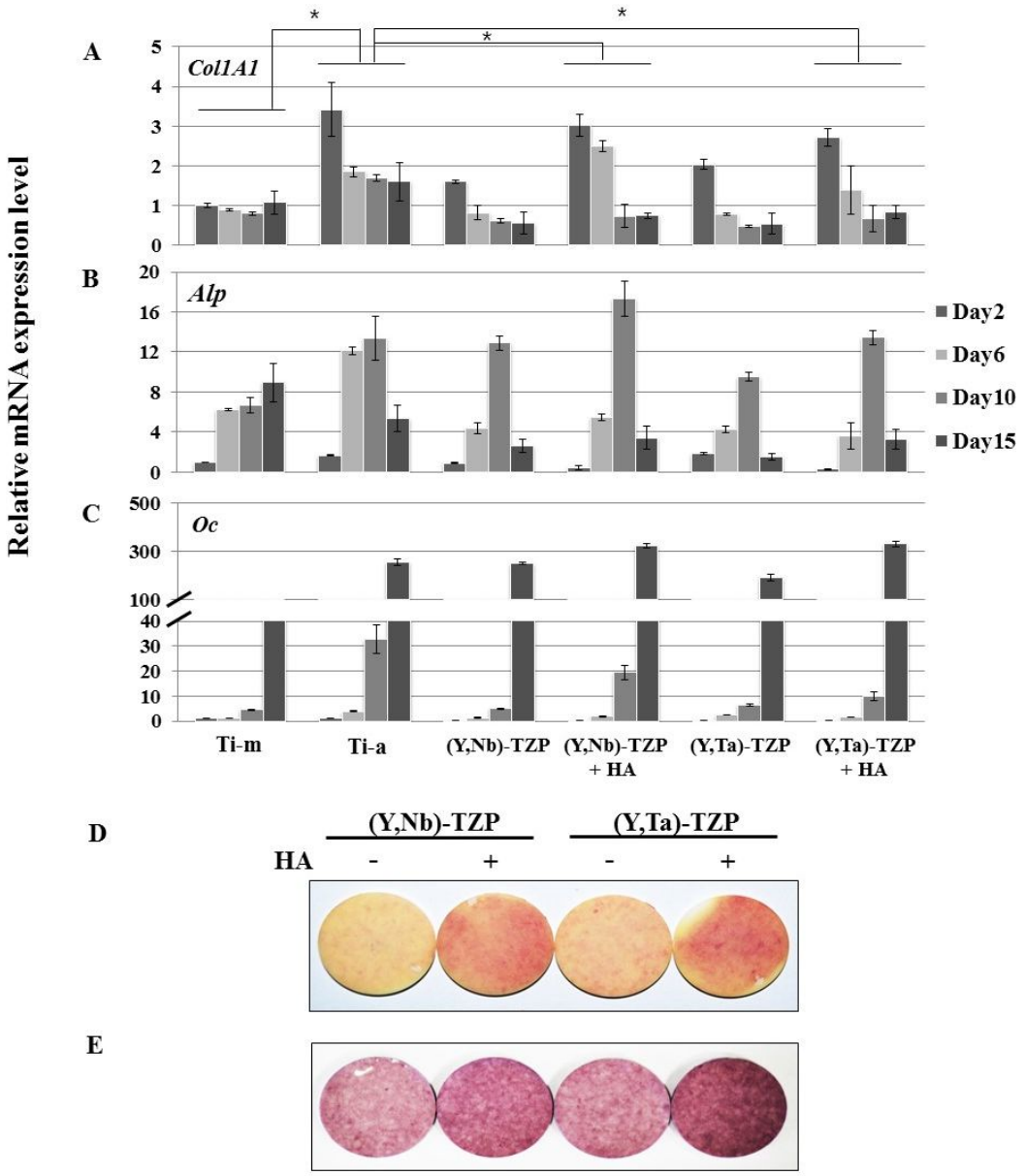

Fig. 7. Real-time PCR. A. type I collagen (*Col1A1*), B. alkaline phosphatase (*Alp*), and C. osteocalcin (*Oc*) in MC3T3-E1 cells on Ti or Zr discs after 2, 6, 10 and 15 days of culture in osteogenic medium. The data are expressed as the mean ± SD of three independent experiments. * Significant differences between groups ($p < 0.05$). D. ALP staining. Cells were seeded on the discs and cultured in osteogenic medium for 7 days. ALP activity was determined by cytochemical staining as indicated under "Materials and methods". E. Alizarin red S staining. Cells were seeded on the discs and cultured in osteogenic medium for 21 days. Staining procedure is stated in the "Materials and methods"

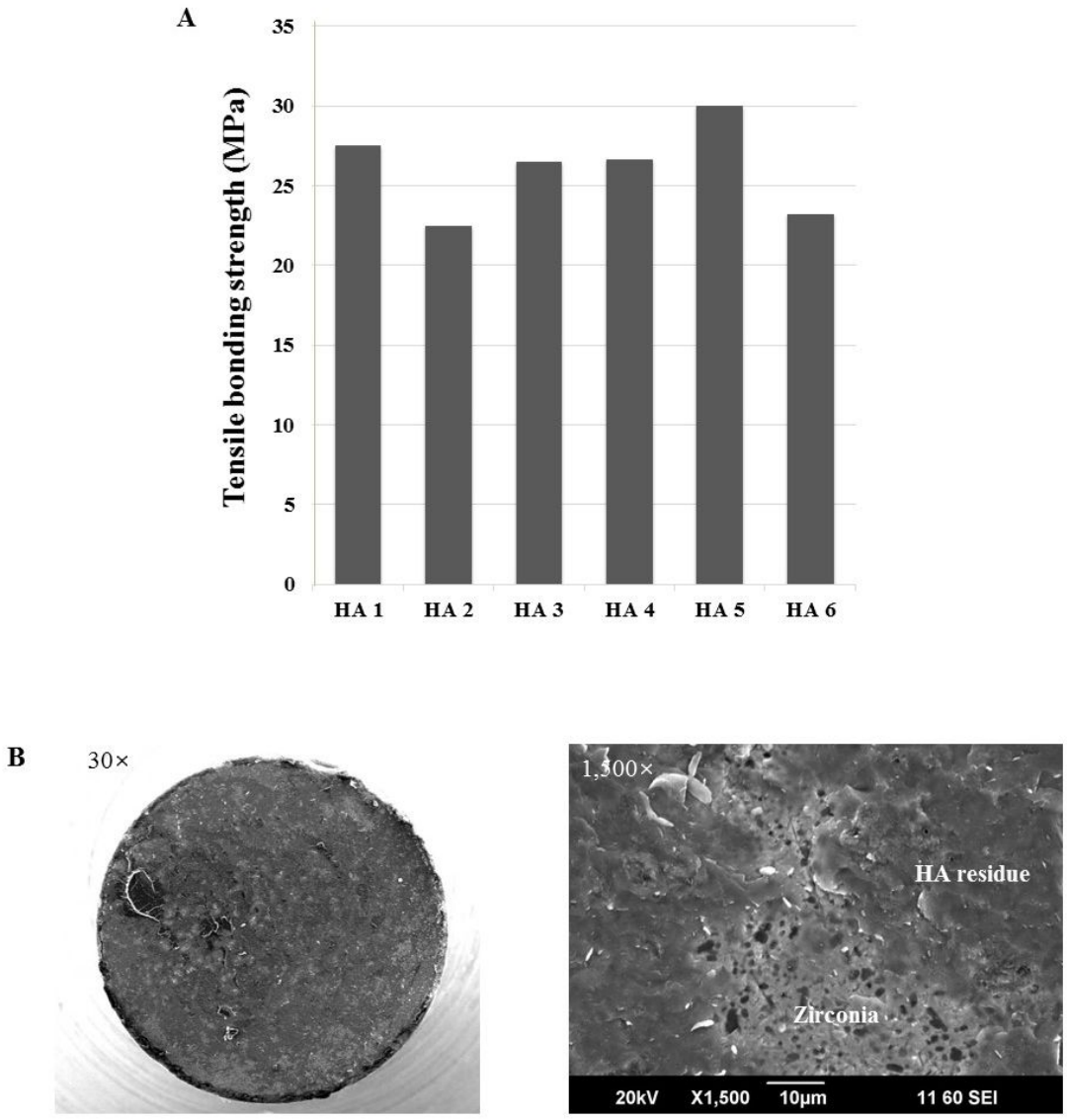

Fig. 8. A. Zirconia-HA tensile bonding strength. B. SEM photographs of the fractured surface between HA coating and zirconia substrate. Images are magnified 30× (left) and 1,500× (right). HA residue was observed on the zirconia surface.

국문초록

에어로졸 분사 방식을 이용한 수산화인회석 코팅 지르코니아의 골형성 반응 및 결합강도에 관한 연구

서울대학교 대학원 치의과학과 치과보철학 전공

(지도교수 한 중 석)

홍 진 선

연구목적: 본 연구의 목적은 상온에서 에어로졸 분사 기술을 이용하여 지르코니아 표면에 수산화인회석 코팅한 표면의 특성 및 결합강도를 조사하고 이에 대한 골반응 능력을 평가하는 것이다.

재료 및 방법: 직경 15㎜, 두께 1㎜의 (Y, Nb)-TZP, (Y, Ta)-TZP 두 종류의 지르코니아 디스크를 제작한 후 수산화인회석 분말을 에어로졸 분사 방식을 이용하여 10 ㎛ 두께로 코팅하였다. 제작된 시편의 평균 표면 거칠기(R_a)와 접촉각을 각각 현미경(CLSM)과 자동 접촉각 측정장치로 측정하였다. 결정 구조와 결합 강도는 각각 X-선 회절법과 ASTM C-633 측정방식에 따라 만능 시험기로 측정하였다. 지르코니아와 티타늄 디스크에서 세포 분화능은 Picogreen assay로 분석하였다. MC3T3-E1 전골아세포 분화 후 2일, 6일, 10일, 15일에 type I collagen, alkaline phosphatase, osteocalcin에 대한 정량적 real-time PCR을 시행하여 골표지 유전자 발현을 측정하였다. 수산화인회석 코팅의 결합강도는 만능시험기를 이용하여 인장강도를 측정하였으며, 파절된 면을 주사전자현미경으로 관찰하였다. 지르코니아 디스크의 접촉각과 평균 표면 거칠기(R_a)는 t 검정을 적용하였고, 티타늄 디스크와 지르코니아 디스크에서 세포분화능력, 세포독성, 정량적 real time PCR은 일원배치 분산분석(ANOVA) 및 사후검정을 적용하여 분석하였다.

결과: 공초점 레이저 현미경과 X-선 회절법으로 관찰한 수산화인회석 코팅 지르코니아 디스크는 균일하고 치밀한 수산화인회석 코팅 두께를 나타내었다. 수산화인회석 코팅 지르코니아 표면의 접촉각은 수산화인회석을 코팅하지 않은 지르코니아 표면의 접촉각 보다 유의하게 낮았다($p < 0.001$). 공기분사 방식에 의한 수산화인회석 코팅의 표면 거칠기는 유의하게 증가하였다($p < 0.05$). MC3T3-E1 전골아세포 부착은 티타늄과 지르코니아 디스크에서 유의한 차이를 보이지 않았으나, ALP, alizarin red S 염색을 통해 수산화인회석 코팅 지르코니아 표면에서 수산화인회석이 코팅되지 않은 지르코니아 디스크 보다 높은 골형성 능력을 확인하였다.

결론: 본 실험적 연구에서 다음의 결론을 얻었다.

1. 공기 분사방식을 이용한 수산화인회석 코팅 후 화학적 성분변화는 관찰되지 않았다.
2. 수산화인회석이 코팅된 지르코니아 표면의 접촉각은 코팅되지 않은 지르코니아 보다 유의하게 낮았다.
3. 수산화인회석 코팅된 지르코니아 디스크의 표면 거칠기는 유의하게 증가되었다.
4. 지르코니아 디스크 표면에 세포 부착은 티타늄 디스크와 유사하였다.
5. 수산화인회석이 코팅된 지르코니아 디스크는 티타늄 디스크와 유사하거나 약간 높은 골형성 반응을 나타내었다.
6. 지르코니아와 수산화인회석 코팅의 결합강도는 평균 26.02MPa ± 3.92 였다.

본 실험적 연구에서, 공기 분사방식을 이용한 수산화인회석 코팅은 우수한 표면 거칠기 향상을 나타내었으며, 이는 골형성에 유리한 효과를 보였다. 다만, 골융합에 대한 수산화인회석 코팅 지르코니아 임플란트의 효과를 확인하기 위한 추가적인 in vivo 연구가 필요할 것으로 사료된다.

주요어: 임플란트, 수산화인회석 코팅 지르코니아, 골형성, 표면 특성, 골융합

학번: 2010-31211